

Modeling slump of concrete with fly ash and superplasticizer

I-Cheng Yeh*

Department of Information Management, Chung-Hua Univ. Hsin Chu, Taiwan 30067, R.O.C.

(Received January 1, 2008, Accepted July 18, 2008)

Abstract The effects of fly ash and superplasticizer (SP) on workability of concrete are quite difficult to predict because they are dependent on other concrete ingredients. Because of high complexity of the relations between workability and concrete compositions, conventional regression analysis could be not sufficient to build an accurate model. In this study, a workability model has been built using artificial neural networks (ANN). In this model, the workability is a function of the content of all concrete ingredients, including cement, fly ash, blast furnace slag, water, superplasticizer, coarse aggregate, and fine aggregate. The effects of water/binder ratio (w/b), fly ash-binder ratio (fa/b), superplasticizer-binder ratio (SP/b), and water content on slump were explored by the trained ANN. This study led to the following conclusions: (1) ANN can build a more accurate workability model than polynomial regression. (2) Although the water content and SP/b were kept constant, a change in w/b and fa/b had a distinct effect on the workability properties. (3) An increasing content of fly ash decreased the workability, while raised the slump upper limit that can be obtained.

Keywords: fly ash; superplasticizer; workability; artificial neural networks.

1. Introduction

For production of high-performance concrete (HPC) that is characterized by low water-cementitious material ratio and a high dosage of superplasticizer (SP), workability properties may be more complex than that of normal concrete. The effect of superplasticizer on workability has been the subject of many investigations. For example, Faroug, *et al.* (1999) indicated that superplasticizers became less effective with increase in w/c ratio. Malhotra (1984) outlined some research needs to resolve some of the problems associated with the use of superplasticizers in concrete. These include development of new types of superplasticizers in concrete containing low-heat cement and compatibility between superplasticizers and supplementary cementing materials such as fly ash and slag.

In recent years, the use of supplementary cementitious materials, mainly fly ash and blast-furnace slag, has become increasingly common in concrete, that imparts some specific qualities to the composite-cement concrete superior to those of concrete made from ordinary portland cement alone. In the case of HPC, the reasons for their use are even stronger (Aitcin and Neville 1993). When fly ash is incorporated as an additional component, the workability properties are rendered even more complicated. There are few literatures that investigate the effect of fly ash quantity on the behavior

* Corresponding Author, Email: icyeh@chu.edu.tw

of the fresh concrete mix. In these literatures no account is taken of the differences between the water demand of cement and that of the combined cement-fly ash mixture (Yen, *et al.* 1999, Domone and Soutsos 1994, Naik and Ramme 1989, Kwan 2000, Punkki, *et al.* 1996). However, it is true that fly ash modifies the water demand of cement in different ways with potential interactive effects on the other components in concrete (Olek and Diamond 1989).

Slump test measurements are often used to determine workability for use in concrete placing. The relationship between the measured slump and the composition of concrete is normally based on engineers' experience or empirical correlations. These correlations are commonly determined from large amount of laboratory tests. The fresh concrete samples of known composition are prepared in the lab and then their slumps are measured (Goh 1995a).

Although it is very difficult to build the workability model, the more we know about the concrete composition-versus-slump relationship, even under laboratory conditions only, the better we can understand the nature of concrete and how to improve concrete quality.

Modern research in material modeling aims to construct mathematical models to describe the relationship between material behaviors and compositions. However, when there are nonlinearities between the dependent variables and independent variable and interactions between dependent variables, it is very difficult to find an accurate model for simulating material behavior. Artificial neural networks (ANN) provide a fundamentally different approach to the derivation and representation of material behavior relationships (Ghaboussi, *et al.* 1991).

A neural network is a computer model whose architecture essentially mimics the knowledge-acquisition of the human brain. Artificial neural networks may take varied forms and are applicable to a wide variety of problems. A number of applications in material have been proposed by several researchers (Nehdi, *et al.* 2001, Brown, *et al.* 1991, Tang and Yen 2000, Kim, *et al.* 2004, Peng 2002, Stegemann and Buenfeld 2004, Kim, *et al.* 2004, Pratt and Sansalone 1992, Basma, *et al.* 1999, Haj-Ali, *et al.* 2001, Goh 1995b, Nehdi, *et al.* 2001, Yeh 1998a, 1998b, 1999). However, little research has been done on modeling workability of concrete using neural networks.

The basic strategy for developing a neural network for material behavior is to train it with the results of a series experiments on a material. If the experimental results contain the relevant information about the material behavior, then the trained neural network would contain sufficient information about the material behavior (Ghaboussi, *et al.* 1991).

In this approach, using neural networks, the effects of replacing cement by fly ash and of addition of SP on workability of concrete were investigated. The investigation covered concrete mixed at different water contents and water-cementitious material ratios, which contained different replacement percentages of fly ash and SP-cementitious material ratios.

2. Neural networks

Fig. 1 showed a three-layer neural network with m continuously valued inputs, n outputs and one layer of hidden units. It requires continuous differentiable nonlinearities. The following sigmoid logistic nonlinearity is usually used (Haykin 2005, Welstead 1994):

(1) for units in the hidden layer

$$h_k = f(\alpha_k) = \frac{1}{1 + e^{-\alpha_k}} \quad (1)$$

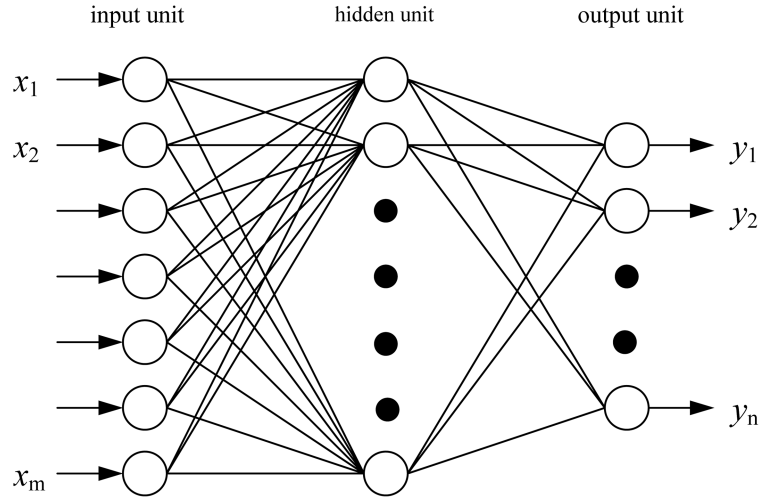


Fig. 1 The architecture of one hidden layer neural network

where α_k is the net value of sum of the product of weights and inputs, i.e.,

$$\alpha_k = \sum_i w'_{ik} \cdot x_i - \theta'_k \quad (2)$$

In the formulas, h_k is the output of nodes in the hidden layer, x_i is the input, w'_{ik} is the connection strengths from the input to the hidden layer, and θ'_k is internal offset in hidden nodes.

(2) for units in the output layer

$$y_j = f(\alpha_j) = \frac{1}{1 + e^{-\alpha_j}} \quad (3)$$

where α_j is the net value of sum of the product of weights and inputs, i.e.,

$$\alpha_j = \sum_k w_{kj} \cdot h_k - \theta_j \quad (4)$$

In the formulas, y_j is the output of nodes in the output layer, w_{kj} is the connection strength from the hidden layer to output layer, and θ_j is internal offset in output nodes.

A thorough treatment of the neural network architecture is beyond the scope of this paper. The basic architecture of neural networks has been covered widely (Haykin 2005, Welstead 1994).

The neural network learns by modifying the weights of the neurons in response to the errors between the actual output values and the target output values. Training pairs are repeatedly presented to the network, and the network adapts its weights using its adaptation formula. The adaptation formula is designed so that each modification of the weights will move the network to a state where it would be more likely to generate the correct response to the current training pair when provided the inputs of that training pair. The adaptation scheme used in this study was the most common one, delta error back propagation (Haykin 2005, Welstead 1994).

The back-propagation training algorithm is an iterative gradient algorithm designed to minimize the mean square error between the actual output of a multilayer feed-forward neural network and the desired output. The basic process of back-propagation training algorithm are summarized as follows (Haykin 2005, Welstead 1994).

Step 1. Initialize weights and offsets

Set all weights and node offsets to small random values.

Step 2. Present input and desired outputs

Present a continuous valued input vector x_0, x_1, \dots, x_{N-1} and specify the desired outputs d_0, d_1, \dots, d_{M-1} .

Step 3. Calculate actual outputs

Use the sigmoid nonlinearity to calculate outputs y_0, y_1, \dots, y_{M-1} .

Step 4. Adapt weights

Use a recursive algorithm starting at the output nodes and work back to the first hidden layer. Adjust weights by

$$w_{ij}(t+1) = w_{ij}(t) + \eta \delta_j x_i' \quad (5)$$

where $w_{ij}(t)$ is the weight from hidden node i or from an input to node j at time t , x_i' is either the output of node i or is an input, η is a gain term, and δ_j is an error term for node j .

(1) If node j is an output node, then

$$\delta_j = y_j(1-y_j)(d_j-y_j) \quad (6)$$

where d_j is the desired output of node j and y_j is the actual output.

(2) If node j is an internal hidden node, then

$$\delta_j = x_j'(1-x_j') \sum_k \delta_k w_{jk} \quad (7)$$

where k is overall nodes in the layer above node j .

Internal node thresholds are adapted in a similar manner by assuming they are connection weights on links from auxiliary constant-valued inputs.

Step 5. Repeat by going to step 2

Repeat by going to Step 2 until convergence is obtained.

The Root Mean Square (*RMS*) error was adopted to provide a measure of the output network performance over the number of training iterations. Moreover, the coefficient of determination (R^2) was adopted as a measure of how well the independent variables considered account for the measured dependent variable. In principle, the higher the R^2 value is, the better the prediction relationship will be.

In the training phase, the neural network being trained is also fed a separate set of data. The neural network predictions using the current trained weights are compared with the target output values. This assesses the reliability of the neural network to generalize correct responses for the

testing patterns that only broadly resemble the data in the training set. No additional learning or weight adjustments occur during this process.

Once the training and testing phases are found to be successful, the neural network can then be put to use in practical applications. The values for the input parameters for the project are presented to the network. Then the network calculates the node outputs using the existing weight values and thresholds developed in the training process (Yen 1999). The neural network will produce almost instantaneous results of the output for the practical inputs provided. The predictions should be reliable, provided the input values are within the range used in the training set (Goh 1995a).

3. Modeling Interactions of fly ash and superplasticizer on workability of concrete

The experimental data include 103 mixtures, which are taken from the tests carried out by Yeh

Table 1 Statistical results of component content in the data set

Component and ratio	Minimum	Maximum	Average	Stdev
Cement (kg)	137.0	374.0	229.9	78.9
Fly Ash (kg)	0.0	193.0	78.0	60.5
Blast Furnace Slag (kg)	0.0	260.0	149.0	85.4
Water (kg)	160.0	240.0	197.2	20.2
Superplasticizer (kg)	4.4	19.0	8.5	2.8
Coarse Aggregate (kg)	708.0	1049.9	884.0	88.4
Fine Aggregate (kg)	640.6	902.0	739.6	63.3
SP/b	0.010	0.038	0.019	0.007
w/b	0.300	0.678	0.461	0.086
fa/b	0.000	0.549	0.171	0.140

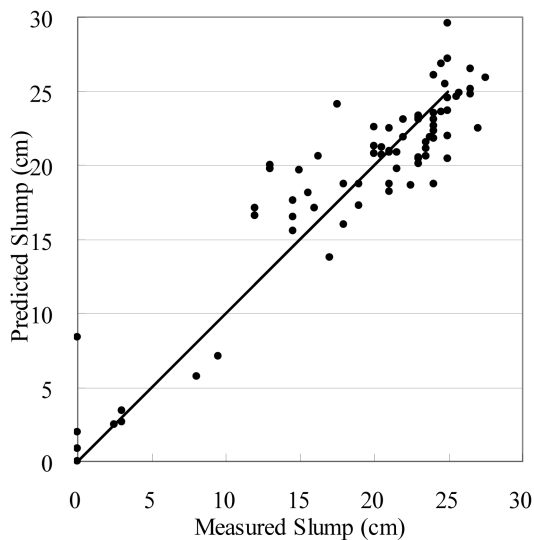


Fig. 2 The measured and predicted slump of neural network for training set

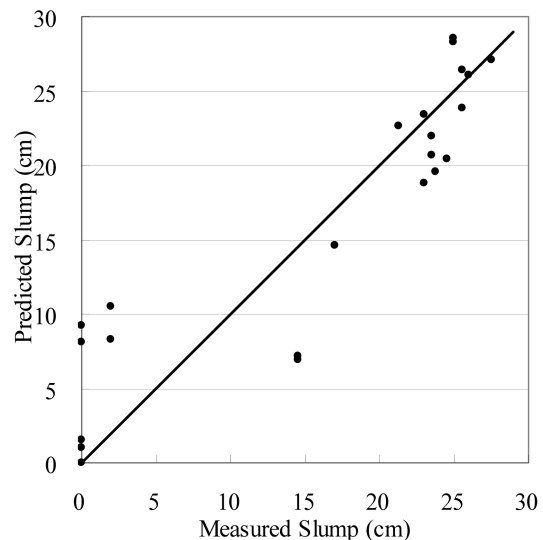


Fig. 3 The measured and predicted slump of neural network for testing set

and Chen (Yeh and Chen 2005). The database of the training and testing data is now available on www.chu.edu.tw/~icyeh/slump_103_data. The statistical results of the data set are listed in Table 1. The workability of fresh concrete was determined by the conventional slump test. These data was randomly divided into training set (78 data) and testing data (25 data).

For this slump modeling problem the obvious inputs are the component contents of concrete, including cement, fly ash, slag, water, SP, coarse aggregate (CA), and fine aggregate (FA), and the output is the slump of the concrete. That is, the neural network developed in the investigation has seven units in the input layer and one unit in the output layer.

After a number of trials, the back-propagation neural network with one hidden layer containing three hidden units was selected.

The measured slump collected from the literature is plotted against the predicted slump calculated by the aforementioned neural network model, as shown in Fig. 2 and Fig. 3. Although the correlation between the measured slump and the predicted values obtained from testing data are somewhat more scattered than that obtained from training data, it is obvious that rather small scatter of data around the diagonal line confirms the fact that neural network is an excellent predictor of the slump.

For comparison purpose, the same training set and testing set are used to build and assess the polynomial regression model. The following polynomial regression formula was adopted here:

$$E(y) = \sum_{i=1}^q \beta_i x_i + \sum_{i=1}^q \sum_{i < j}^q \beta_{ij} x_i x_j \quad (8)$$

where x_i is the i th-component content; β_i and β_{ij} are the regression coefficients.

The measured slump collected from the literature is plotted against the predicted slump calculated by the regression model, as shown in Fig. 4 and Fig. 5. The correlation between the measured slump and the predicted values, obtained from training data, is rather high. However, that obtained

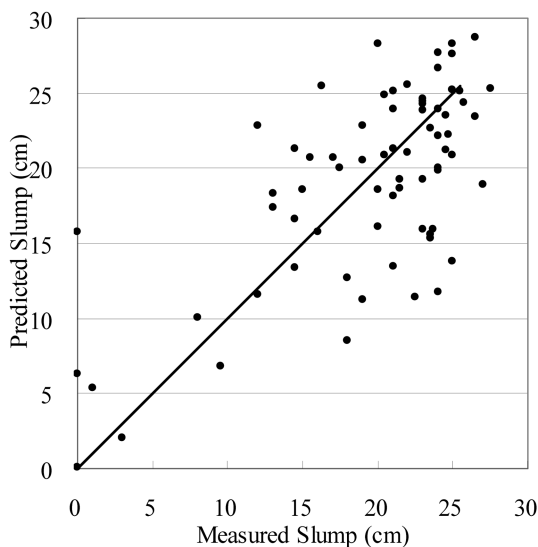


Fig. 4 The measured and predicted slump of polynomial regression for training set

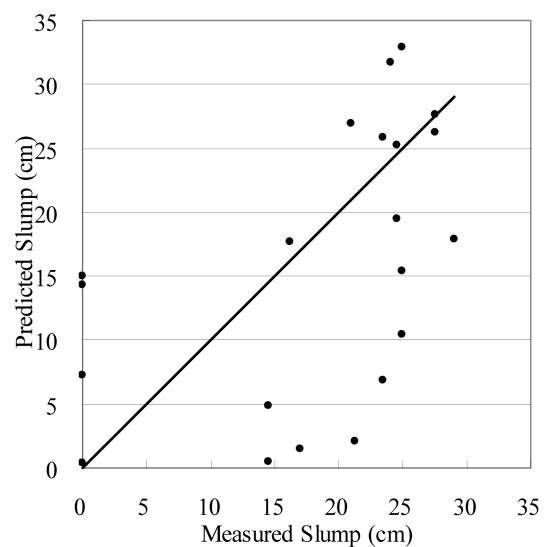


Fig. 5 The measured and predicted slump of polynomial regression for testing set

from testing data is rather low, which indicates the fact that regression is not an excellent predictor of the slump.

Moreover, the value of *RMS* error of neural network model is 2.7 cm for the training set and 4.5 cm for the testing set. It was found that the R^2 value is 0.880 for the training set and 0.830 for the testing set. These indicate a near correlation between the independent variables and the measured dependent variable.

For comparison purpose, the values of *RMS* error (and R^2) of regression model for the training and testing results were also calculated as 5.3 cm (and 0.719) and 10.3 cm (and 0.407), respectively. It is seen that the neural network model gives smaller *RMS* error and the larger R^2 for both training set and testing set, especially for testing set.

4. Analyzing Interactions of fly ash and superplasticizer on workability of concrete

In this study, the variation in concrete slump was achieved by varying combinations of factors like the water/binder ratio, fly ash-binder ratio, SP-binder ratio, and water content. The binder means cementitious material, that is, cement plus fly ash and slag. The range of each variable is listed as follows:

1. The amount of superplasticizer by weight of binder (water-binder ratio, w/b) was varied with 0.3, 0.4, 0.5, 0.6, and 0.7.
2. The amount of superplasticizer by weight of binder (SP-binder ratio, SP/b) was varied with 0, 1, 2, 3, and 4%.
3. The amount of fly ash by weight of binder (fly ash-binder ratio, fa/b) was varied with 0, 10, 20, 30, 40, and 50%.
4. The amount of water was varied from 130 to 250 kg/m³.

Besides, the CA/FA was kept constant 1.3 and the total volume of concrete was 1.000 m³.

From the water content-slump curves generated using the trained neural network developed in this study with the above combinations, some sets of curves has been selected, as shown in Figs. 6 to 14, to explore the effects of fly ash and SP. Figs. 6 to 8 illustrates the water content slump curves with cement paste containing 0 to 50% fly ash with 0% SP/b , while with $w/b=0.3$, 0.5, and 0.7, respectively. Figs. 9 to 11, and Figs. 12 to 14 illustrate the same curves, while with 2% and 4% SP/b , respectively. The corresponding 3D views of these curves are shown in Figs. 15 to 23. Considering the fact that validity of a slump test is generally recommended for concrete with a slump value ranging from 2.5 to 21 cm; therefore, these parts of curves that outside the above range may be unreliable and should be ignored. It was found that

4.1. The effect of w/b

- (1) As seen in Figs. 6 to 14, at high w/b (0.7), with the same SP/b , the shape of slump curve of fly ash concrete is similar to that of pure portland cement concrete. However, at low w/b (0.3), they are rather different.
- (2) At medium w/b (0.5) and high w/b (0.7), all the shape of curves with fly ash show similar increment from the curve without fly ash, but curves for lower w/b show a larger increment than those for higher w/b .

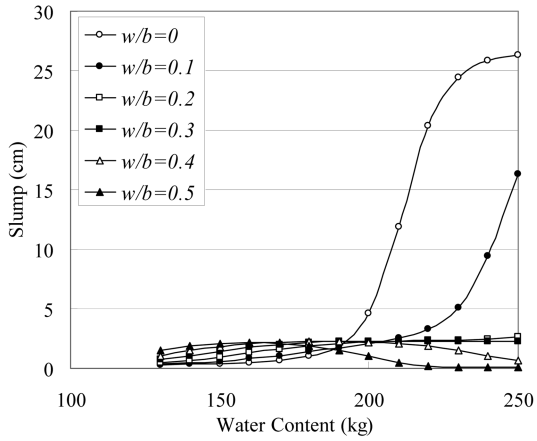


Fig. 6 The water content-slump curves at $w/b=0.3$, $SP/b=0\%$

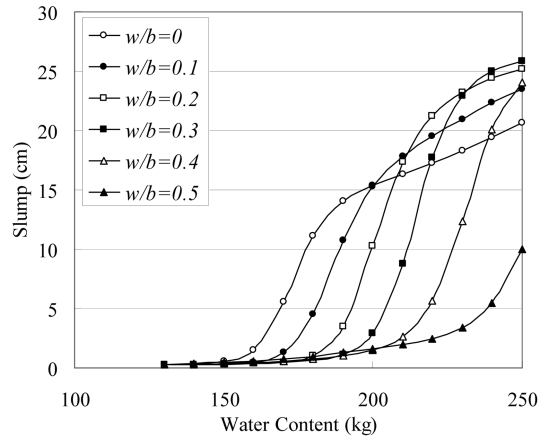


Fig. 7 The water content-slump curves at $w/b=0.5$, $SP/b=0\%$

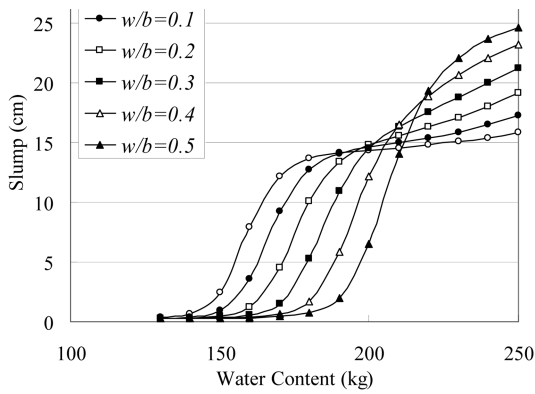


Fig. 8 The water content-slump curves at $w/b=0.7$, $SP/b=0\%$

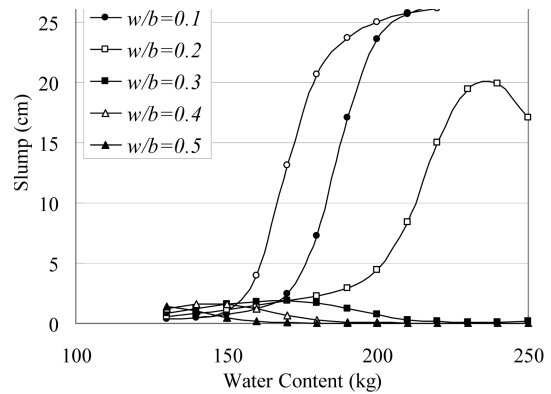


Fig. 9 The water content-slump curves at $w/b=0.3$, $SP/b=2\%$

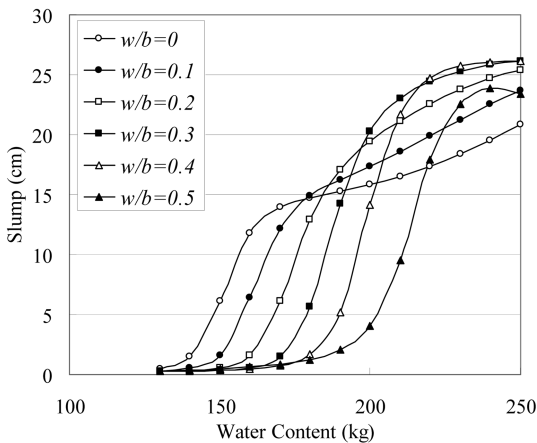


Fig. 10 The water content-slump curves at $w/b=0.5$, $SP/b=2\%$

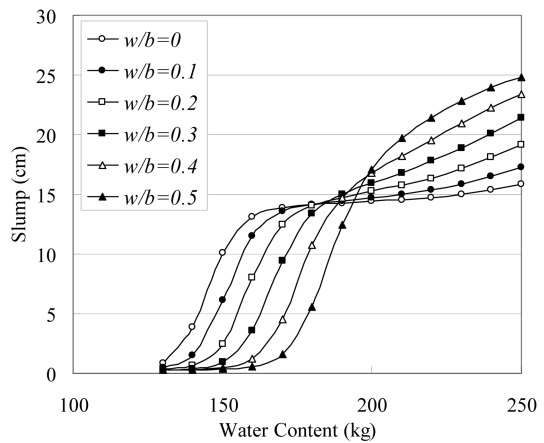


Fig. 11 The water content-slump curves at $w/b=0.7$, $SP/b=2\%$

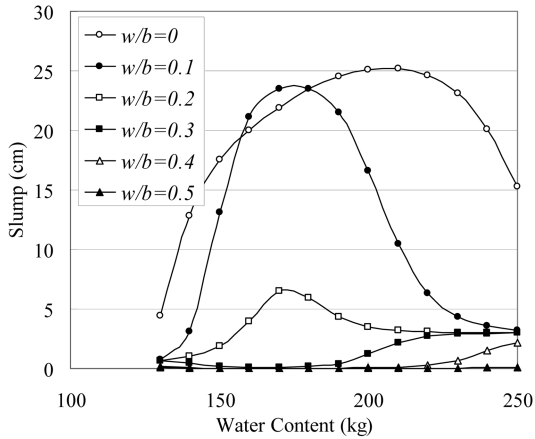


Fig. 12 The water content-slump curves at $w/b=0.3$, $SP/b=4\%$

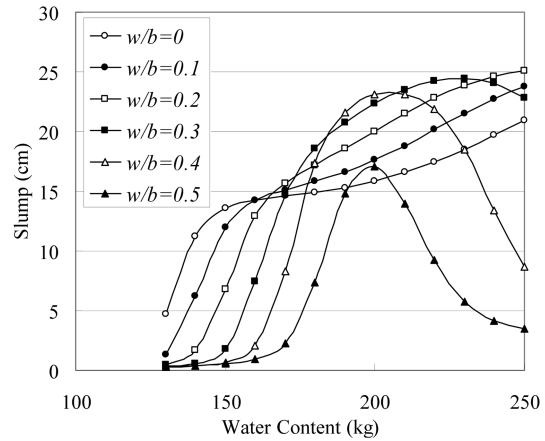


Fig.13 The water content-slump curves at $w/b=0.5$, $SP/b=4\%$

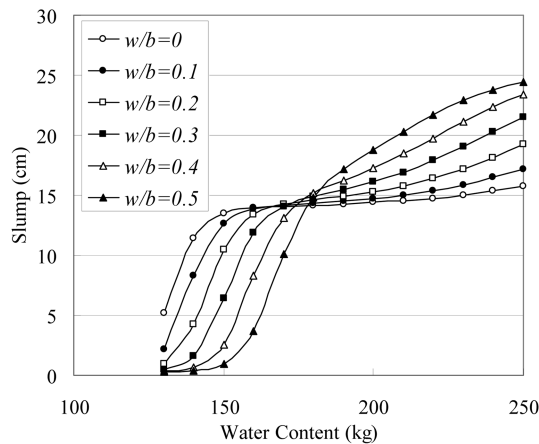


Fig. 14 The water content-slump curves at $w/b=0.7$, $SP/b=4\%$

4.2. The effect of SP/b

- (1) As seen in Figs. 6, 9 and 12, at low w/b (0.3), a greater SP/b ratio can effectively lowers the water content required for pure portland cement concrete to reach high workability. Concrete containing fly ash also exhibits this same tendency. A greater SP/b ratio can effectively lowers the water content required for concrete containing fly ash to reach high workability. For example, at $fa/b=10\%$, at $SP/b=0$ (Fig. 6) and 4% (Fig. 12), the water content required to reach 10 cm in slump is 210 kg/m^3 and 140 kg/m^3 , respectively. The SP/b has large effects on the effects of fa/b on slump.
- (2) As seen in Figs. 8, 11, and 14, at high w/b (0.7), although they show similar tendency, the effects of SP/b decreased.

4.3. The effect of fa/b

- (1) As seen in Figs. 8, 11, and 14, at high w/b (0.7), with high water content (250 kg/m^3), the concrete without fly ash cannot reach a slump higher than 15 cm; however, the concrete with 30% fly ash can reach a slump higher than 20 cm. Hence, fly ash is very useful in concrete mixtures at high w/b (0.7) because it can raise the slump upper limit that can be reached. The results may be explained by that fly ash-binder ratio reflects the quality of cement paste, and affects the flowability of the aggregate particles.
- (2) The slump of concrete is influenced by many factors, the primary factor being water content and SP/b ratio. This study indicated that if the fly ash was incorporated in the concrete, in general, the water content required to reach a given slump was increased, while the slump upper limit that can be obtained was raised. The effect may be explained by the SP absorbing effect of the fly ash particles. It should be noted, however, that for the present concrete mixes, the dosage of SP was based on weight of binder. One unit weight of fly ash may absorb more SP than one unit weight of cement. As a result, an increased amount of fly ash will increase the required amount of SP.

4.4. The effect of water content

- (1) At $w/b=0.3$ (Figs. 6, 9, and 12), without SP, it is very difficult to reach a high slump larger than 20 cm under water content lower than 210 kg/m^3 , while with $SP/b=2\%$ and 4% , it is possible to reach a high slump (20 cm) under water content higher than 180 and 160 kg/m^3 , respectively.
- (2) At $w/b=0.7$ (Figs. 8, 11, and 14), there is a 15 cm upper bound on slump for the concrete without fly ash; however, there is no such bound for the concrete with 30% and above fly ash.
- (3) As can be seen in Figs. 15 to 23, there is a lower limit water content to start to produce slump, and the lower limit dependent on w/b , SP/b , and fa/b . The lower w/b , SP/b and the higher fa/b , then, the higher the lower limit water content to start to produce slump.

5. Conclusions

Workability is often expressed in terms of slump, which reflects the most conventional way of describing the workability properties of fresh concrete. In the present paper, the feasibility of using neural network models for evaluating workability of concrete containing fly ash and SP was investigated. The neural networks were used to explore the model. After learning from a set of randomly selected patterns, the neural network model was able to produce reasonably accurate predictions for patterns not included in the training set. Finally, using the trained network, some information about slump of concrete with a water-binder ratio (water-cementitious material ratio), fly ash-binder ratio (replacement percentage), SP-binder ratio, and water content in the range of 0.3 to 0.7, 0 to 50%, 0 to 4%, and 130 to 250 kg/m^3 , respectively, is reported.

Considering the fact that validity of a slump test is generally recommended for concrete with a slump value ranging from 25 to 210 mm; therefore, these parts of curves that outside the range may be unreliable and should be ignored. It was found that

1. From the previous discussion, the use of neural network for the modeling of slump of concrete

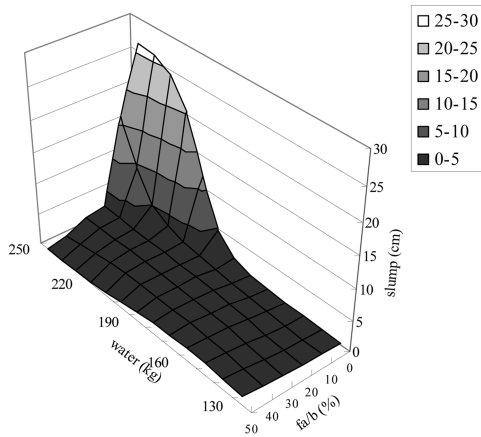


Fig. 15 The 3D view of slump response surface at $w/b=0.3, SP/b=0\%$

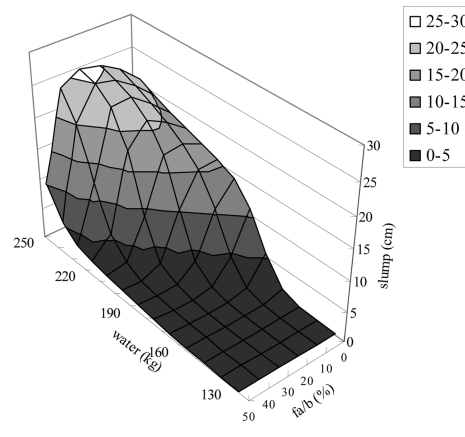


Fig. 16 The 3D view of slump response surface at $w/b=0.5, SP/b=0\%$

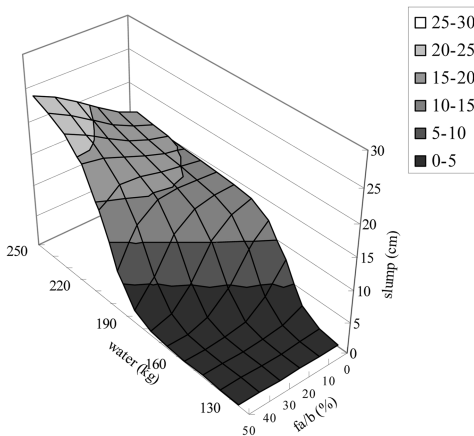


Fig. 17 The 3D view of slump response surface at $w/b=0.7, SP/b=0\%$

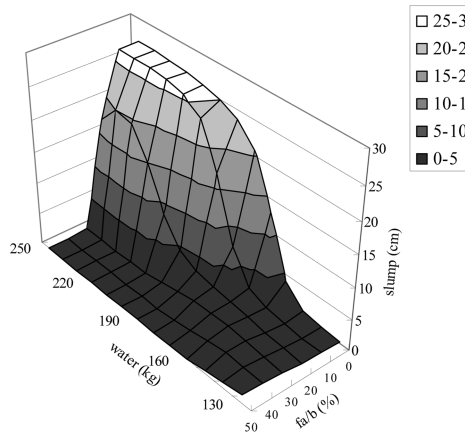


Fig. 18 The 3D view of slump response surface at $w/b=0.3, SP/b=2\%$

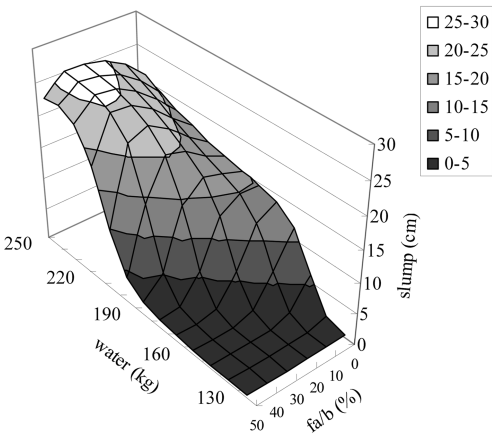


Fig. 19 The 3D view of slump response surface at $w/b=0.5, SP/b=2\%$

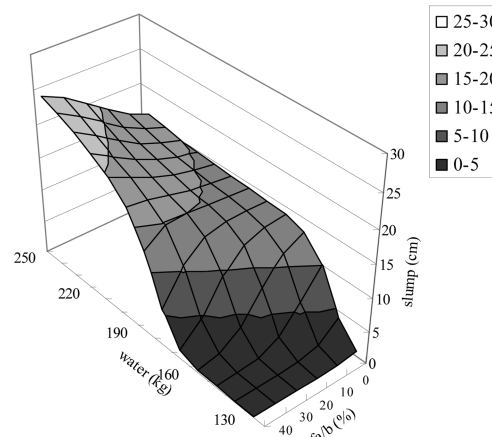


Fig. 20 The 3D view of slump response surface at $w/b=0.7, SP/b=2\%$

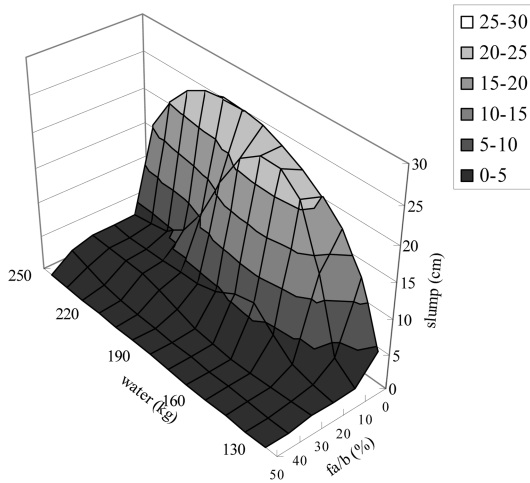


Fig. 21 The 3D view of slump response surface at $w/b=0.3$, $SP/b=4\%$

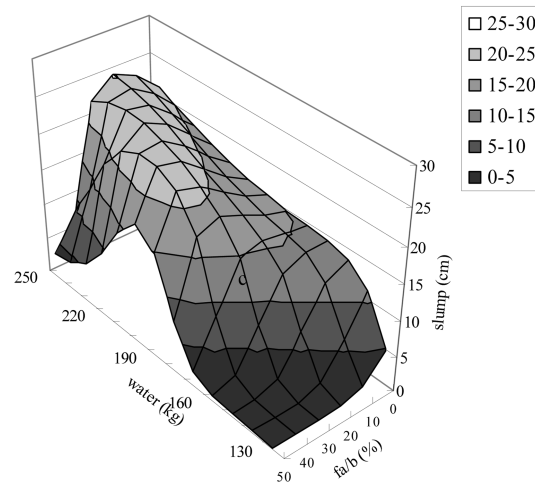


Fig. 22 The 3D view of slump response surface at $w/b=0.5$, $SP/b=4\%$

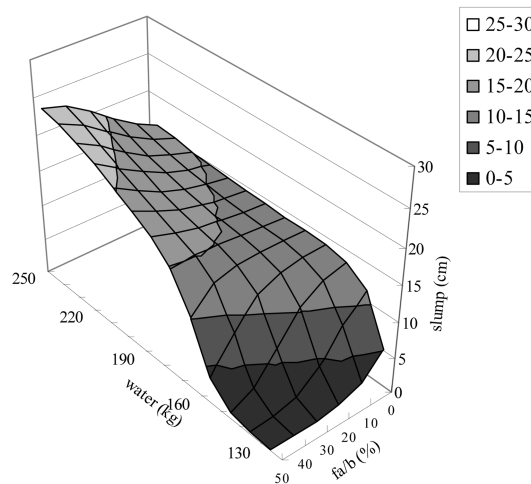


Fig. 23 The 3D view of slump response surface at $w/b=0.7$, $SP/b=4\%$

containing fly ash and superplasticizer looks very promising.

2. Although the water content and SP/b ratio were kept constant, Figs. 6 to 14 demonstrates that a change in w/b ratio and fa/b ratio had a distinct effect on the workability properties.

3. Incorporating fly ash increased the water content required to obtain a given slump, while raised the slump upper limit that can be obtained. At $w/b=0.5$, and $SP/b \geq 2\%$, 30 to 50% fly ash replacement had beneficial effect on the slump of concrete.

4. In the light of the results of this study, the appropriateness of common design practice treating the workability properties of all concretes as functions of its water content and SP/b ratio only, regardless of the constitution of cementitious materials and paste should be reconsidered. In case of high volume fly ash concrete, the effect of fly ash on the workability properties of concrete should be thoroughly investigated and if possible incorporated in the future concrete design codes.

5. Finally, this study focused only on the effects of fly ash content on the slump. The effects of slag content or the effects on workability loss should also be further investigated.

Acknowledgments

This work was supported by the National Science Council, ROC, under Grant NSC-97-2221-E-216-038.

References

- Aitcin, P.-C. and Neville, A. (1993), "High-performance concrete demystified", *Concrete Int.*, Jan. 1993, 21-26.
- Basma, A.A., Barakat, S., and Al-Oraimi, S. (1999), "Prediction of cement degree of hydration using artificial neural networks", *ACI Mater. J.*, **96**(2), 167-172.
- Brown, D.A., Murthy, P.L. N., and Berke, L. (1991), "Computational simulation of composite ply micromechanics using artificial neural networks", *Microcomputers in Civ. Eng.*, **6**(2), 87-97.
- Domone, P.L.J. and Soutsos, M.N. (1994). "An approach to the proportioning of high-strength concrete mixes", *Concr. Int.*, October 1994, 26-31.
- Faroug, F., Szwaborski, J., and Wild, S. (1999), "Influence of superplasticizers on workability of concrete", *J. Mater. Civ. Eng.*, **11**(2), 151-157.
- Ghaboussi, J., Garrett, J.H., and Wu, X. (1991), "Knowledge-based modeling of material behavior with neural networks", *J. Eng. Mech.*, **117**(1), 132-153.
- Goh, A.T.C. (1995a), Neural networks for evaluating CPT calibration chamber test data", *Micro. Civ. Eng.*, **10**(2), 147-151.
- Goh, A.T.C. (1995b), "Prediction of ultimate shear strength of deep beams using neural networks", *ACI Struct. J.*, **92**(1), 28-32.
- Haj-Ali, R.M., Kurtis, K.E., and Akshay, R. (2001), "Neural network modeling of concrete expansion during long-term sulfate exposure", *ACI Mater. J.*, **98**(1), 36-43.
- Haykin, S. (2005), *Neural Networks: A Comprehensive Foundation*, Prentice Hall PTR, NJ.
- Kim, H., Rauch, A.F., and Haas, C. T. (2004), "Automated quality assessment of stone aggregates based on laser imaging and a neural network", *J. Comput. Civil Eng.*, **18**(1), 58-64.
- Kim, J.-I., Kim, D.K., Feng, M. Q., and Yazdani, F. (2004), "Application of neural networks for estimation of concrete strength", *J. Mater. Civil Eng.*, **16**(3), 257-264.
- Kwan, A.K.H. (2000), "Use of condensed silica fume for making high-strength, self-consolidating concrete". *Can. J. Civil Eng.*, **27**(4), 620-627.
- Malhotra, V.M. (1984), "Superplasticizers: reducing water in concrete", *Civil Eng.-ASCE*, **54**(12), 56-59.
- Naik, T.R. and Ramme, B.W. (1989), "High-strength concrete containing large quantities of fly ash", *ACI Mater. J.*, **86**(2), 110-116.
- Nehdi, M. Djebbar, Y., and Khan, A. (2001), "Neural network model for preformed- foam cellular concrete", *ACI Mater. J.*, **98**(5), 402-409.
- Nehdi, M., El-Chabib, H., and El-Naggar, M.H. (2001), "Predicting performance of self-compacting concrete mixtures using artificial neural networks", *ACI Mater. J.*, **98**(5), 394-401.
- Olek, J. and Diamond, S. (1989), "Proportioning of constant paste composition fly ash concrete mixes", *ACI Mater. J.*, **86**(2), 159-166.
- Peng, J., Li, Z., and Ma, B. (2002), "Neural network analysis of chloride diffusion in concrete". *J. Mater. Civil Eng.*, **14**(4), 327-333.
- Pratt, D. and Sansalone, M. (1992), "Impact-echo signal interpretation using artificial intelligence", *ACI Mater. J.*, **89**(2), 178-187.
- Punkki, J., Golaszewski, J., and Gjorv, O.E. (1996), "Workability loss of high-strength concrete", *ACI Materials*

- J.*, **93**(5), 427-431.
- Stegemann, J.A. and Buenfeld, R.N. (2004), "Mining of existing data for cement-solidified wastes using neural networks", *J. Environ. Eng.*, **130**(5), 508-515.
- Tang, C.-W. and Yen, T. (2000), "Prediction of the ultimate shear strength of high-and normal-strength concrete beams without stirrups using neural networks". in High Strength/High Performance Concrete, Konig, G. *et al.* (eds), **1**, 595-608.
- Welstead, S.T. (1994), "Neural network and fuzzy logic applications in C/C++", John Wiley & Sons, New York.
- Yeh, I-Cheng. (1998a), "Modeling concrete strength with augment-neuron networks", *J. Mater. Civil Eng.*, **10**(4), 263-268.
- Yeh, I-Cheng. (1998b), "Modeling of strength of high performance concrete using artificial neural networks", *Cement Concrete Res.*, **28**(12), 1797-1808.
- Yeh, I-Cheng. (1999), "Design of high performance concrete mixture using neural networks and nonlinear programming", *J. Comput. Civil Eng.*, **13**(1), 36-42.
- Yeh, I-Cheng and Chen, J.W. (2005), "Modeling workability of concrete using design of experiments and artificial neural networks", *J. Technol.*, **20**(2), 153-162.
- Yen, T., Tang, C.-W., Chang, C.-S., and Chen, K.-H. (1999), "Flow behaviour of high strength high-performance concrete", *Cement Concrete Comp.*, 1999, **21**(5), 413-424.